catalysts

MDPI

Article

Byproduct Analysis of SO_2 Poisoning on NH_3-SCR over $MnFe/TiO_2$ Catalysts at Medium to Low Temperatures

Tsungyu Lee and Hsunling Bai *

Institute of Environmental Engineering, National Chiao Tung University, Hsinchu 300, Taiwan; ashley.ev98g@nctu.edu.tw

* Correspondence: hlbai@nctu.edu.tw; Tel.: +886-3-5731868; Fax: +886-3-5725958

Received: 18 February 2019; Accepted: 11 March 2019; Published: 15 March 2019

Abstract: The byproducts of ammonia-selective catalytic reduction (NH_3-SCR) process over $MnFe/TiO_2$ catalysts under the conditions of both with and without SO_2 poisoning were analyzed. In addition to the NH_3-SCR reaction, the NH_3 oxidation and the NO oxidation reactions were also evaluated at temperatures of 100–300 °C to clarify the reactions occurred during the SCR process. The results indicated that major byproducts for the NH_3 oxidation and NO oxidation tests were N_2O and NO_2, respectively, and their concentrations increased as the reaction temperature increased. For the NH_3-SCR test without the presence of SO_2, it revealed that N_2O was majorly from the NH_3-SCR reaction instead of from NH_3 oxidation reaction. The byproducts of N_2O and NO_2 for the NH_3-SCR reaction also increased after increasing the reaction temperature, which caused the decreasing of N_2-selectivity and NO consumption. For the NH_3-SCR test with SO_2 at 150 °C, there were two decay stages during SO_2 poisoning. The first decay was due to a certain amount of NH_3 preferably reacted with SO_2 instead of with NO or O_2. Then the catalysts were accumulated with metal sulfates and ammonium salts, which caused the second decay of NO conversion. The effluent N_2O increased as poisoning time increased, which was majorly from oxidation of unreacted NH_3. On the other hand, for the NH_3-SCR test with SO_2 at 300 °C, the NO conversion was not decreased after increasing the poisoning time, but the N_2O byproduct concentration was high. However, the SO_2 led to the formation of metal sulfates, which might inhibit NO oxidation reactions and cause the concentration of N_2O gradually decreased as well as the N_2-selectivity increased.

Keywords: Selective Catalytic Reduction (SCR); SO_2 poisoning; Low-temperature catalyst; nitrogen oxides; nitrous oxide

1. Introduction

Nitrogen oxides (NO_x, NO and NO_2) produced from stationary sources are major air pollutants that lead to environmental concerns such as photochemical smog and acid rain [1]. The most effective technology for the removal of NO_x emission from coal-fired power plants is ammonia-selective catalytic reduction (NH_3-SCR; SCR hereafter) [2]. The traditional SCR catalysts are active within the temperature window of 300–400 °C [3,4]. Even though some of the traditional catalyst compositions such as V_2O_5–WO_3/ TiO_2 or Fe-zeolite-based catalysts can lower down their working temperature window to be as low as 250 or even 200 °C [5–10], there is still a strong demand in developing SCR catalysts to be active at less than 200 °C and placing them downstream of the electrostatic precipitator and desulfurizer [11–13].

Literature data showed that Mn-based catalysts have good activity for low-temperature SCR [14–17]. Moreover, in iron containing SCR catalysts, the introduction of Mn could obviously

enhance the low-temperature activity, probably due to the fact that synergistic effect between iron and manganese species [18]. It was reported that the MnFe/TiO_2 could improve the activity, stability and SO_2 durability of the SCR catalysts using NH_3 as the reducing agent [19–23].

In the past, there have been extensive studies usingFourier-transform infrared spectroscopy (FTIR) for understanding the mechanism of SCR reaction on the surface of MnFe catalysts [24–28]. In addition, several different types of reaction mechanisms have been proposed including the typical Eley–Rideal mechanism and Langmuir–Hinshelwood mechanism. For the Eley–Rideal mechanism, it is assumed that the gaseous NO directly reacts with an activated ammonia surface complex [29]. On the other hand, the Langmuir–Hinshelwood reaction mechanism involves that a surface NO complex reacts with an activated ammonia [3,30]. Moreover, Yang et al. [31] used in situ diffuse reflectance infrared Fourier transform spectroscopy (DRIFTS-FTIR) to reveal the mechanism of low-temperature SCR reaction over the MnFe spinel. The results indicated that the contribution of Eley–Rideal mechanism to NO conversion increased after increasing the reaction temperature.

Although many studies have been done on the SCR mechanism, to the authors' best knowledge, there has been no work on clarifying reactions occurred in the medium to low-temperature SCR system with and without the presence of SO_2. Therefore, this study employed MnFe/TiO_2 catalyst to study the oxidation of NH_3, the oxidation of NO and the NH_3-SCR reaction with and without the presence of SO_2 at 100–300 °C. The reactants and byproducts of gaseous NO, NH_3, N_2O, and NO_2 in the effluent streams as well as solid byproducts of ammonium salts and metal sulfates on the catalysts were analyzed. The results can offer useful information to understand the reaction pathway at different operation conditions for the application of medium to low-temperature SCR catalysts.

2. Results and Discussion

2.1. Oxidation Reactions of NH_3 and NO without SO_2

To understand the products and byproducts of oxidation reactions, the NH_3 and NO oxidation reactions over the MnFe/TiO_2 catalyst were studied within the temperature range of 100–300 °C, which was the most active temperature region for MnFe/TiO_2 catalyst in SCR reaction [32]. In addition, the N-balance of NH_3 and NO oxidation tests were calculated by Equations (1) and (2), respectively.

$$\text{N-balance in } NH_3 \text{ oxidation} = \frac{[NH_3]_{out} + [N_2O]_{out} + [NO]_{out} + [NO_2]_{out}}{[NH_3]_{in}} \times 100\% \quad (1)$$

$$\text{N-balance in NO oxidation} = \frac{[NO]_{out} + [NO_2]_{out}}{[NO]_{in}} \times 100\% \quad (2)$$

The results of N-balance and outlet gas concentrations in the NH_3 oxidation reaction without SO_2 over MnFe/TiO_2 catalyst at different reaction temperatures are shown in Figure 1. It can be seen that the major oxidation product of NH_3 was N_2O (i.e., Equation (3) shown later in the Materials and Method section) instead of NO (Equation (4)). In addition, N_2O increased from 31 ppm to 219 ppm after increasing the reaction temperature from 100 °C to 300 °C. On the other hand, the effluent NO concentration was only 36 ppm at most, which occurred at reaction temperature of 300 °C; but no NO_2 was found in the effluent at all tested temperatures.

The results of N-balance and outlet gas concentrations in the NO oxidation reaction over MnFe/TiO_2 catalyst at different reaction temperatures are shown in Figure 2, it can be seen that NO could be oxidized to NO_2, and the concentration of NO_2 was significantly increased from 10 to 309 ppmv for reaction temperatures from 100 to 300 °C.

The above results indicated that NH_3 and NO oxidations (Equations (3)–(5)) increased after increasing the reaction temperature, and the major products of NH_3 oxidation and NO oxidation were N_2O and NO_2, respectively. In addition, it can be observed that both the N-balance results shown in Figures 1 and 2 were very high at 97~100% in the 100–300 °C range. This indicates that we can detect almost all the reaction species.

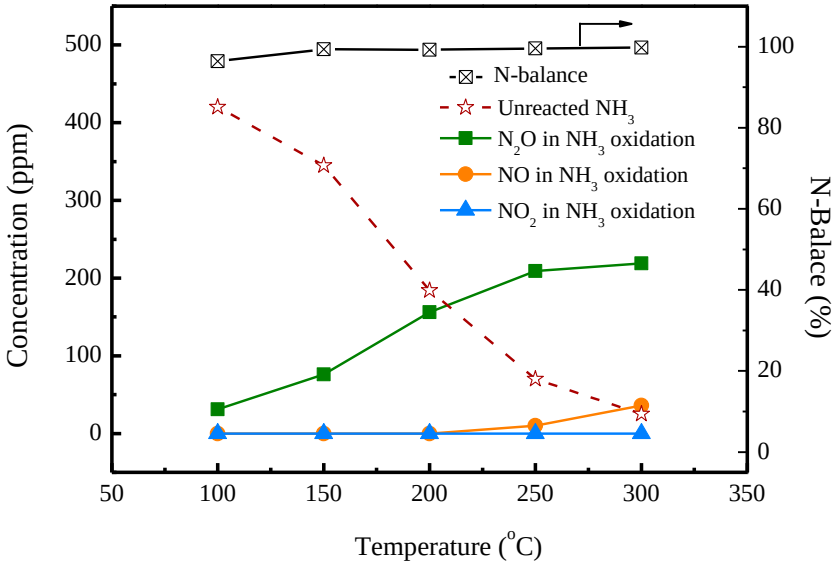

Figure 1. N-balance and outlet gas concentrations in the NH_3 oxidation reaction without SO_2 over $MnFe/TiO_2$ catalyst at different reaction temperatures. Reaction conditions: [NH_3] = 500 ppm, [O_2] = 10%, balanced with N_2, GHSV = 50,000 h^{-1}.

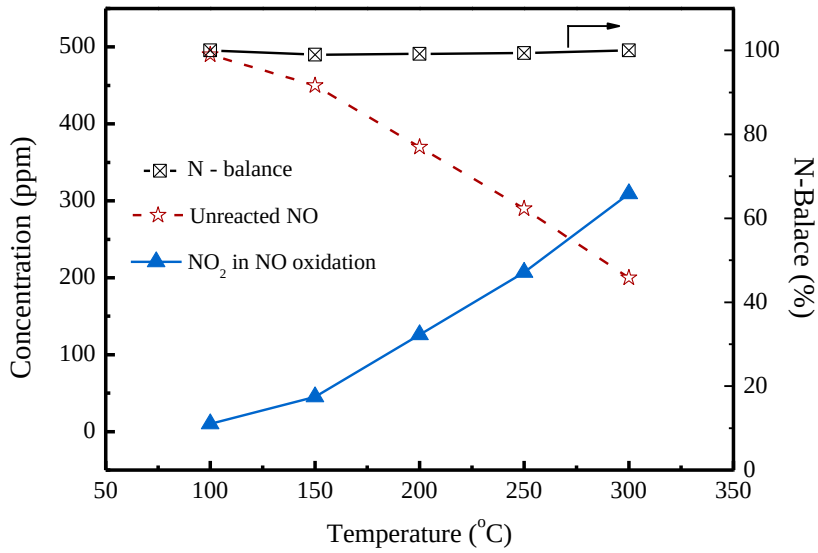

Figure 2. N-balance and outlet gas concentrations in the NO oxidation reaction without SO_2 over $MnFe/TiO_2$ catalyst at different reaction temperatures. Reaction conditions: [NO] = 500 ppm, [O_2] = 10%, balanced with N_2, GHSV = 50,000 h^{-1}.

2.2. SCR Reactions without SO_2

Figure 3 shows the NO consumption (in ppmv) and outlet gas concentrations of N_2O, NO_2 and NH_3 over the $MnFe/TiO_2$ catalyst for reaction temperatures of 100–300 °C. It can be seen that the $MnFe/TiO_2$ catalyst maintained high NO consumption in the SCR reaction. When raising reaction temperature from 100 to 200 °C, the NO consumption in the SCR reaction increased slightly from 450 ppm to 495 ppm, and the outlet concentration of NH_3 was slightly decreased from 63 to 0 ppm.

At the reaction temperature of 200 °C, the concentrations of N_2O and NO_2 were 175 and 0 ppm, respectively, with 98% of NO consumption in the SCR reactions (500 ppm NO reacted with 500 ppm NH_3). On the other hand, the N_2O from NH_3 oxidation (500 ppm NH_3 reacted with O_2) at the reaction temperature of 200 °C was 156 ppm (as indicated by Figure 1). Therefore, it can be seen

that in the SCR system, lower N_2O percentage ($\frac{175\text{ppm } N_2O}{500\text{ ppm NO} + 500\text{ ppm } NH_3}$ = 17.5%) was being produced as compared to that during only NH_3 oxidation ($\frac{156\text{ ppm } N_2O}{500\text{ ppm } NH_3}$ = 31.2%).

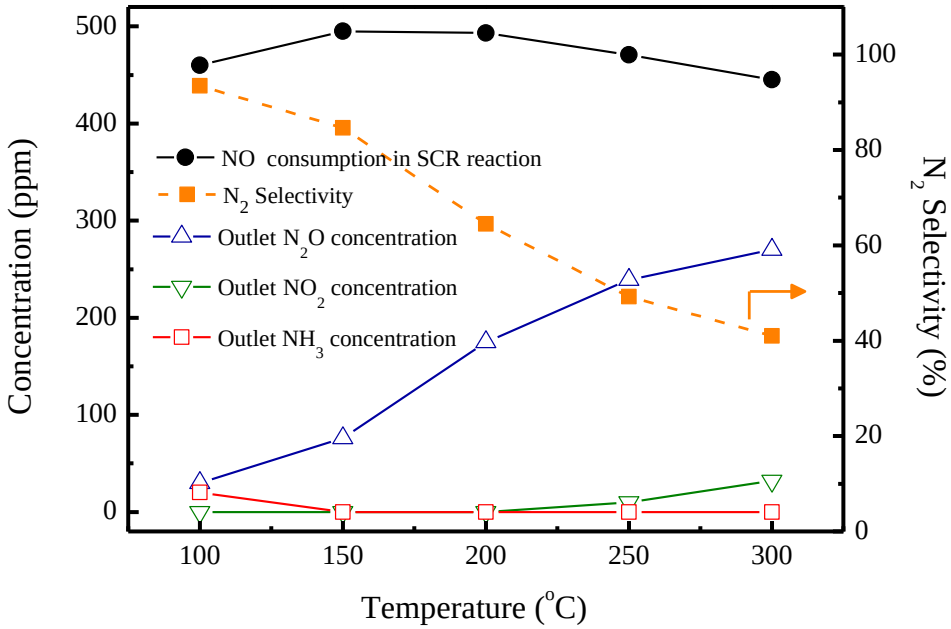

Figure 3. NO consumption and outlet gas concentrations in the NH_3-SCR reaction without SO_2 over MnFe/TiO_2 catalyst at different reaction temperatures. Reaction conditions: Reaction temperature = 100~300 °C, [NO] = 500 ppm, [NH_3] = 500 ppm, [O_2] = 10%, balanced with N_2, and GHSV = 50,000 h^{-1}.

The "fast SCR" (Equation (8)), first proposed in 1986 [33], proceeds at a much higher reaction rate than "standard SCR" reactions (Equations (6) and (7)) was developed to improve deNO_x efficiency at lower temperatures [34,35]. As indicated by Figure 2 for the NO oxidation reaction, NO could be oxidized to NO_2 at temperatures higher than 150 °C, but NO_2 was not detected at temperature below 200 °C in the SCR test as seen in Figure 3. This might be due to the fact that NO_2 would react with NO and NH_3 according to the fast SCR reaction (Equation (8)).

After further raising the reaction temperature from 200 to 300 °C, NO consumption in the SCR reaction was slightly decreased from 495 ppm to 455 ppm, and concentrations of N_2O and NO_2 increased from 175 to 270 ppm and 0 to 36 ppm, respectively. When reaction temperature increased, oxidation reactions occurred more quickly as indicated by Figures 1 and 2. Hence the reason for slight decreases in the NO consumption at above 200 °C might be due to the fact that NO was oxidized (Equation (5)) as also demonstrated in the literature [26,36–38]. Moreover, the results of Figure 3 also indicated that products of the SCR reaction gradually changed from N_2 to N_2O when raising the temperature from 100 to 300 °C. Therefore, the N_2-selectivity of SCR reaction was gradually decreased from 93% to 41% after increasing the reaction temperature from 100 °C to 300 °C.

2.3. SCR Reactions with SO_2

To clarify the byproducts of SCR reactions with SO_2, NO consumption in the SCR reaction and outlet gas concentrations in the NH_3-SCR reaction over MnFe/TiO_2 catalyst at 150 and 300 °C are shown in Figure 4a,b, respectively. It can be seen in Figure 4a that there were four stages during the SCR test period. At stage I where no SO_2 was introduced, the NO consumption in the SCR reaction was very high (495 ppm out of 500 ppm). After 150 ppm SO_2 was introduced, the NO consumption in the SCR reaction decreased rapidly within 60 min SO_2 poisoning (stage II), and they remained roughly stable for another 60 min (stage III), then decreased gradually with time again (stage IV).

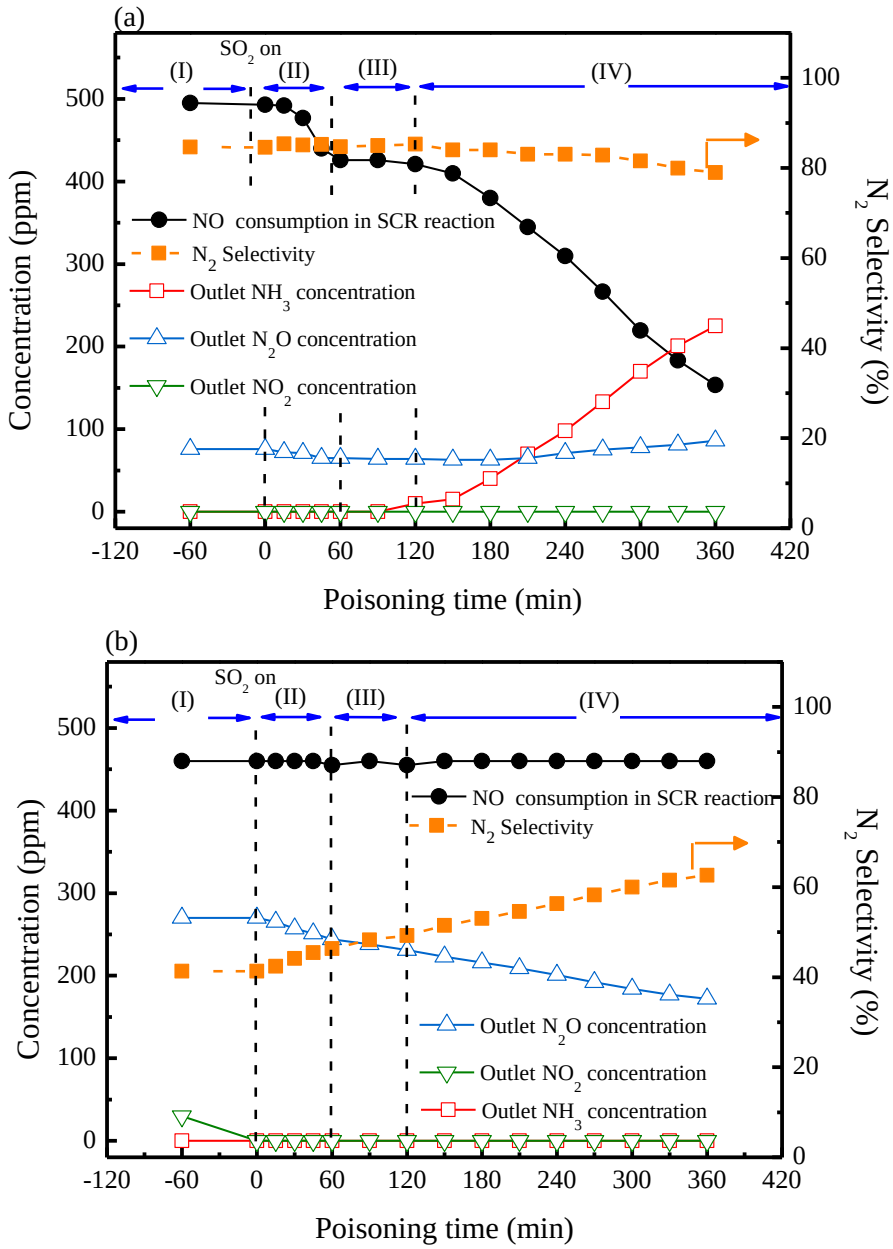

Figure 4. NO consumption and outlet gas concentrations in the NH_3-SCR reaction with SO_2 over $MnFe/TiO_2$ catalyst at (**a**) 150 °C and (**b**) 300 °C. Reaction conditions: [NO] = 500 ppm, [NH_3] = 500 ppm, [SO_2] = 150 ppm, [O_2] = 10%, balanced with N_2, and GHSV = 50,000 h^{-1}.

In our previous work [32], it was found that the gradual decrease (stage II) of NO consumption in the SCR reaction was probably due to the fact that SO_2 competed with NO to react with NH_3 and form ammonium salts. However, the $MnFe/TiO_2$ catalyst still had good activity at stage III. Thus, during this stage, there was no sufficient NH_3 to react with NO, which caused NO consumption remained relatively lower but stable at around 425 ppm from 60 to 120 min SO_2 poisoning time as compared to stages I and II. At stage IV, NO consumption in the SCR reaction decreased significantly from 420 ppm to 153 ppm for poisoning time from 120 to 360 min, which was due to accumulation of metal sulfates and ammonium salts which blocked the active sites of catalyst.

On the other hand, no effluent NH_3 was detected from stage I to stage III. Then NH_3 slip occurred at stage IV as seen in Figure 4a, which was due to less active sites and decreasing NO consumption in the SCR reaction. One can also see that concentrations of N_2O slightly decreased from 76 to 63 ppm within 120 min SO_2 poisoning time (stage II and III), then increased gradually to 86 ppm after

360 min SO_2 poisoning time (stage IV). This result indicated that SO_2 would react with NH_3 and form ammonium salts, which cause concentrations of N_2O slightly decreased at stages II and III. Then NH_3 slip occurred at stage IV, which caused increasing N_2O concentrations.

For the SCR test with SO_2 at 300 °C as shown in Figure 4b, it can be seen that the SO_2 poisoning effect was negligible as compared to the poisoning test at low temperature. When the reaction temperature was at 300 °C, the NO consumption in the SCR reaction remained around 460 ppm, which was almost the same as those without SO_2 poisoning. Moreover, during the SCR activity tests no SO_2 concentration was detected, which indicated that all the gas phase SO_2 molecules might be adsorbed and/or reacted with metal catalysts.

The main reason for the inhibition of SO_2 poisoning might be attributed to different SCR reaction mechanisms at different temperatures. Literature results showed that at lower temperatures (<200 °C), SCR reactions would follow the Langmuir−Hinshelwood mechanism. In the Langmuir−Hinshelwood mechanism, SO_2 would compete with NO to be adsorbed on the active sites, which cause the decreases of SCR efficiencies. However, when reaction temperature increased, the SCR reaction mechanism would transform from Langmuir−Hinshelwood mechanism to Eley–Rideal mechanism. In the high temperature range (>200 °C), the SCR reaction mainly followed the Eley–Rideal mechanism, over which the gaseous NO could directly react with an activated ammonia [30,39,40].

One can also see from Figure 4b that at reaction temperature of 300 °C, the SCR system did not have NH_3 slip. The concentrations of NO_2 and N_2O decreased from 30 to 0 ppm and from 270 to 172 ppm, respectively; and the N_2-selectivity increased from 41% to 62% for the SCR reaction from stage II to stage IV. The result indicated that by increasing the reaction temperature to 300 °C the SO_2 poisoning effect could be inhibited, and the N_2 selectivity can be enhanced due to the decreased N_2O concentrations.

The amount of sulfate species on the catalysts was estimated by thermo-gravimetric analysis (TGA) analysis and the results are shown in Figure 5 in terms of differential thermogram (DTG) spectra. The weight loss profiles of all samples showed three distinct decomposition steps: (1). the weight loss at low temperature (<200 °C) was assigned to the water desorption on the catalyst surface. (2). the weight loss at 200–400 °C could be attributed to decomposition of ammonium salts [41–43]. (3). the weight loss at high temperature (>670 °C) was originated from metal sulfates [44,45].

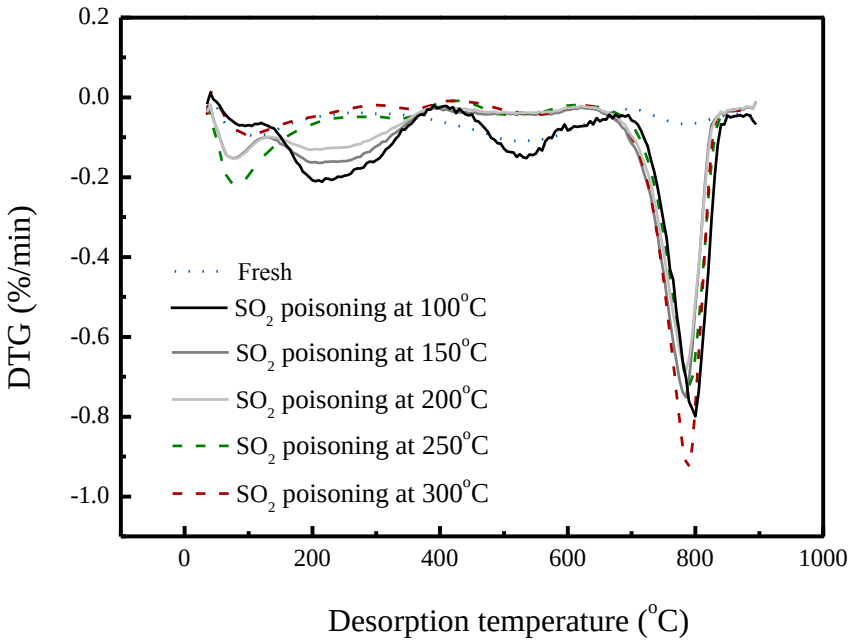

Figure 5. DTG spectra of fresh catalyst and catalysts poisoned at different reaction temperatures after 6 h poisoning time.

It can be seen from Figure 5 that the fresh catalyst had only one major weight loss peak, which appeared at 50–150 °C and corresponded to H_2O desorption on the catalyst surface. On the other hand, decomposition peaks of both ammonium salts (200–400 °C) and metal sulfates (670–900 °C) were observed on all MnFe/TiO_2 catalysts poisoned at temperature ranges of 100–200 °C. When reaction temperatures were 250 °C and 300 °C, there were no decomposition peak of ammonium salts. This reveals that ammonium salts were not formed on the catalyst surface at temperatures above 250 °C. As also noted in Figure 5, there was another peak in the range of temperature of 400–600 °C for the fresh catalyst and poisoned catalyst at 100 °C. However, since we cannot find related literature discussed on this, so the reason for this peak is not clear.

The amounts of sulfate species of fresh and poisoned catalysts are listed in Table 1. It is observed that the amounts of ammonium salts on the catalysts decreased from 2.3 wt.% to negligible amounts by increasing the SCR reaction temperature from 100 to 300 °C. This indicated that the reaction temperature would directly affect the formation of ammonium salts. It is noted that rigid quantification of metal sulfates accumulated on the poisoned catalyst was not possible via the DTG data because some ammonium salts could also be transformed into metal sulfates during the continuous TGA heating process [46]. Hence we can only confirm that all the poisoned catalysts had roughly similar amounts of metal sulfates during the temperature from 100 °C to 250 °C (within experimental error of TGA instrument, ±0.3 wt.%), except for the case at 300 °C.

Table 1. Amounts of ammonium salts and metal sulfates deposited on the catalyst surfaces.

MnFe/TiO_2 Poisoned with Different Reaction Temperatures	Ammonium Salts [a] (by weight) %	Metal Sulfates [b] (by Weight) %
Fresh	0.0	0.0
100 °C	2.3	4.21 [c]
150 °C	1.8	4.11 [c]
200 °C	1.1	4.03 [c]
250 °C	0.1	4.08 [c]
300 °C	0(−0.1)	4.52 [c]

[a] The amount of ammonium salts was calculated by weight difference between the fresh and poisoned catalysts from the TGA spectrum of 200–400 °C. [b] The amount of metal sulfates was calculated by weight difference between the fresh and poisoned catalysts from the TGA spectrum of 670–900 °C. [c] Rigid quantification of the amounts of metal sulfates is not possible via the DTG data because it was possible that some of the ammonium salts could transform into metal sulfates during the heating process of TGA.

At high temperature of 300 °C, the NO consumption was not affected by SO_2. Thus, it is easy to predict that adding an excessive amount of NH_3 tends to be oxidized and forming N_2O and NO as observed in Figure 1. However, at low temperature of 150 °C, the NO consumption was significantly affected by SO_2. Thus, to ensure the gradual decrease of NO consumption at stage II of Figure 4a was due to the competition between SO_2 and NO to react with NH_3, different inlet amounts of NH_3 were tested to study the SO_2 poisoning mechanism at temperature of 150 °C. The results are shown in Figure 6. One can see that adding different amounts of NH_3 had a similar effect on NO consumption at stages I and IV; but it had different NO consumptions at stages II and III. On the other hand, the NH_3 outlet concentrations were different at all stages. At stage I, NH_3 only reacted with a certain amount of NO and thus extra NH_3 slip was detected in the outlet gas. When SO_2 was introduced, NH_3 not only reacted with NO but also reacted with SO_2. Therefore, both the outlet concentrations of NH_3 and NO consumption decreased at stages II and III. Besides, when increasing NH_3 amount to above 550 ppm (i.e., NH_3/NO molar ratio of 1.1), the first decay of NO consumption at stage II could be inhibited. This indicated that NH_3 concentration was sufficient to react with NO and SO_2. The result shown in Figure 6 indicated that if a sufficient amount of NH_3 can be provided to react with both SO_2 and NO, then the first decay of NO consumption could be inhibited at early time of stage II. However, after 120 min of SO_2 poisoning (stage IV), the NO consumption could not be affected by different amounts

of NH_3. Thus, the more injection amount of NH_3 led to eventually the more amount of NH_3 slip to the atmosphere.

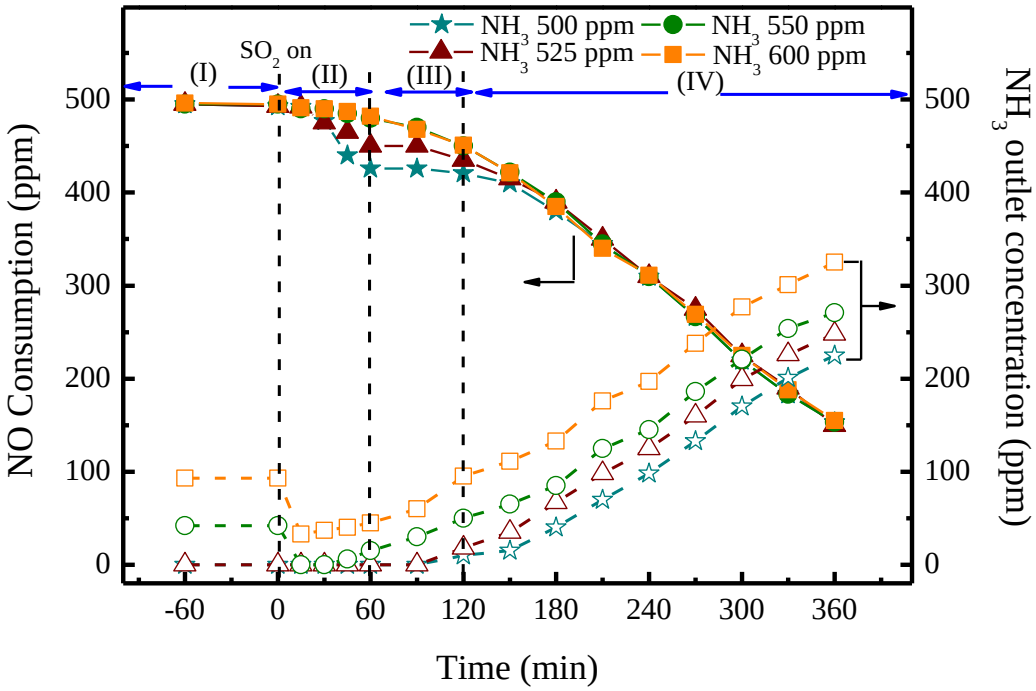

Figure 6. NO consumption and outlet NH_3 concentrations in the NH_3-SCR reaction with SO_2 over $MnFe/TiO_2$ catalyst at different ammonium amounts. Reaction conditions: Reaction temperature = 150 °C, [NO] = 500 ppm, [NH_3] = 500~650 ppm, [SO_2] = 150 ppm, [O_2] = 10%, balanced with N_2, and GHSV = 50,000 h^{-1}.

2.4. Product and Byproduct Analysis

Since different reactions occurred during the SCR process, i.e., Equations (3)–(12), were considered both with and without SO_2, thus the percentages of product and byproducts can be calculated. Table 2 lists formulas for calculating the percentages of N-containing product (N_2) as well as gaseous and solid byproducts (NO, N_2O and salts) formed during the SCR process. The byproducts could be formed by the SCR reaction as well as by the NH_3 oxidation or the NO oxidation reactions. Because it is difficult to clarify that the outlet NO was from NH_3 oxidation or from the unreacted NO, therefore the NO formation from NH_3 oxidation (Equation (4)) is neglected and all the effluent NO was assumed to be only from the unreacted NO. This is an acceptable assumption since the formation of NO from NH_3 oxidation was very minor (0~7%) at reaction temperatures of 100~300 °C as observed from Figure 1. Besides, it was assumed that the fast SCR reaction (Equation (8)) only served as the intermediate reaction at the low temperature SCR process [35]. Thus, the fast SCR reaction was not considered in the calculation of the percentages of all N-containing product and byproducts.

Based on formulas shown in Table 3, the results on percentages of all N-containing species during the NH_3-SCR process tested at 150 °C are shown in Figure 7a; and those tested at 300 °C are shown in Figure 7b. It can be seen from Figure 7a that at SCR operation temperature of 150 °C and without the presence of SO_2, the major product of SCR process appeared to be N_2. This indicated that $MnFe/TiO_2$ catalyst can serve as a good catalyst and achieve high N_2 selectivity at low temperature of 150 °C when SO_2 was not presented in the system. The minor presence of N_2O byproduct in the exhaust was majorly from the SCR reaction rather than from the NH_3 oxidation reaction.

Table 2. Formulas for calculating the N-containing product and byproduct percentages during the SCR process.

Product and Byproduct	Reaction Equation	Percentage Calculation Equation
NO_2	**NO oxidation to NO_2 (Equation (5)):** $2NO + O_2 \rightarrow 2NO_2$	**The percentage of NO_2 from NO oxidation** $[NO_2]_{NO}\ (\%) = [\frac{[NO_2]_{out}}{[NO]_{in}+[NH_3]_{in}}] \times 100\%$
Salts $(NH_4)_2SO_4$ NH_4HSO_4	**Ammonium salts** **Equations (10) and (11):** $SO_3 + 2NH_3 + H_2O\ (NH_4)_2SO_4$ $SO_3 + NH_3 + H_2O \rightarrow NH_4HSO_4$	**The percentage of salts** $[Salt](\%) = [\frac{[NH_3]_{Salt}{}^{\#}}{[NO]_{in}+[NH_3]_{in}}] \times 100\%$ #the NH_3 consumption of salts reaction ($[NH_3]_{Salt}$) were indicated by result of Figure 6
N_2O	**NH_3 slip oxidation to form N_2O** **$[N_2O]_{slip}$ (%)**	**The percentage of N_2O from NH_3 slip oxidation** $[N_2O]_{slip}\ (\%) = [\frac{[NH_3]_{out} \times \frac{[N_2O]}{[NH_3]}{}^{*}}{[NO]_{in}+[NH_3]_{in}}] \times 100\%$ * $\frac{[N_2O]}{[NH_3]}$: from results of NH_3 oxidation test (Figure 1)
	NH_3 oxidation to form N_2O **Equation (3):** $2NH_3 + 2O_2 \rightarrow N_2O + 3H_2O$	**The percentage of N_2O from NH_3 oxidation** $[N_2O]NH_3\ (\%) = 1 - [\frac{2[NO]_{SCR}}{[NO]_{in}+[NH_3]_{in}}] \times 100\% - [NO_2]_{NO}(\%) - [Salt](\%) + [N_2O]_{Slip}(\%)$
	SCR reaction to form N_2O **Equation (7):** $4NO + 4NH_3 + 3O_2 \rightarrow 4N_2O + 6H_2O$	**The percentage of N_2O from SCR reaction** $[N_2O]SCR\ (\%) =$ $[\frac{2[N_2O]_{out}}{[NO]_{in}+[NH_3]_{in}}] \times 100\% - [N_2O]_{NH3}(\%)$
N_2	**SCR reaction to form N_2** **Equation (6):** $4NO + 4NH_3 + O_2 \rightarrow 4N_2 + 6H_2O$	**The percentage of N_2 from SCR reaction** $[N_2]SCR\ (\%) =$ $[\frac{2[NO]_{SCR}}{[NO]_{in}+[NH_3]_{in}}] \times 100\% - [N_2O]_{SCR}(\%)$

On the other hand, when SO_2 was introduced at 150 °C, the percentages of N_2 and N_2O decreased after increasing the poisoning time as observed in Figure 7a. Because NH_3 could not be reacted with NO due to decreased availability of active sites, it tends to increase the NO and NH_3 slip to the atmosphere. In addition, the portion of N_2O from NH_3 oxidation was also gradually increased as increasing the SO_2 poisoning time. After 360 min of SO_2 poisoning, the exhaust N_2O from NH_3 oxidation was more than from SCR reaction. One can also see that percentages of ammonium salts were similar at different SO_2 poisoning times. This indicated that certain amounts of NH_3 would preferentially be reacted with SO_2. In addition, the remaining NH_3 would then be reacted with NO or O_2. Moreover, it can be seen that percentages of NO slip were higher than percentages of NH_3 slip at different SO_2 poisoning times, which is due to the fact that NH_3 not only reacted with NO but also reacted with SO_2 and O_2.

For results at 300 °C as seen in Figure 7b, it is observed that NO_2 from NO oxidation disappeared during the SO_2 poisoning. However, the unreacted NO (NO slip) appeared during the SO_2 poisoning. This indicated that the formation of metal sulfates at 300 °C might inhibit the NO oxidation reaction. At high temperature, the SCR reaction mainly followed the Eley–Rideal mechanism, so the continuous decreasing of N_2O concentration as poisoning time increases and no SO_2 concentration in the outlet gases might be related to the reaction between SO_2 and activated NH_3 instead of the NH_3 oxidation reaction at 300 °C. Moreover, the total percentages of N_2 and N_2O from SCR reactions remained almost the same no matter SO_2 was presented in the system or not. The low N_2 selectivity revealed that $MnFe/TiO_2$ catalyst may not be a good candidate for SCR process at 300 °C unless the space velocity can be reduced to further enhance the more complete reduction of NO to N_2 instead of forming the N_2O byproduct. However, it is interested to note that the N_2 selectivity gradually increased and the percentages of N_2O from SCR reaction gradually decreased after increasing SO_2 poisoning time. This indicated that SO_2 promotion phenomenon might exist at 300 °C, which was attributed to the formation of $SO_4{}^{2-}$ on the catalyst surface. This increased NH_3 adsorption and promoted NH_3 reaction with NO via Eley−Rideal mechanism.

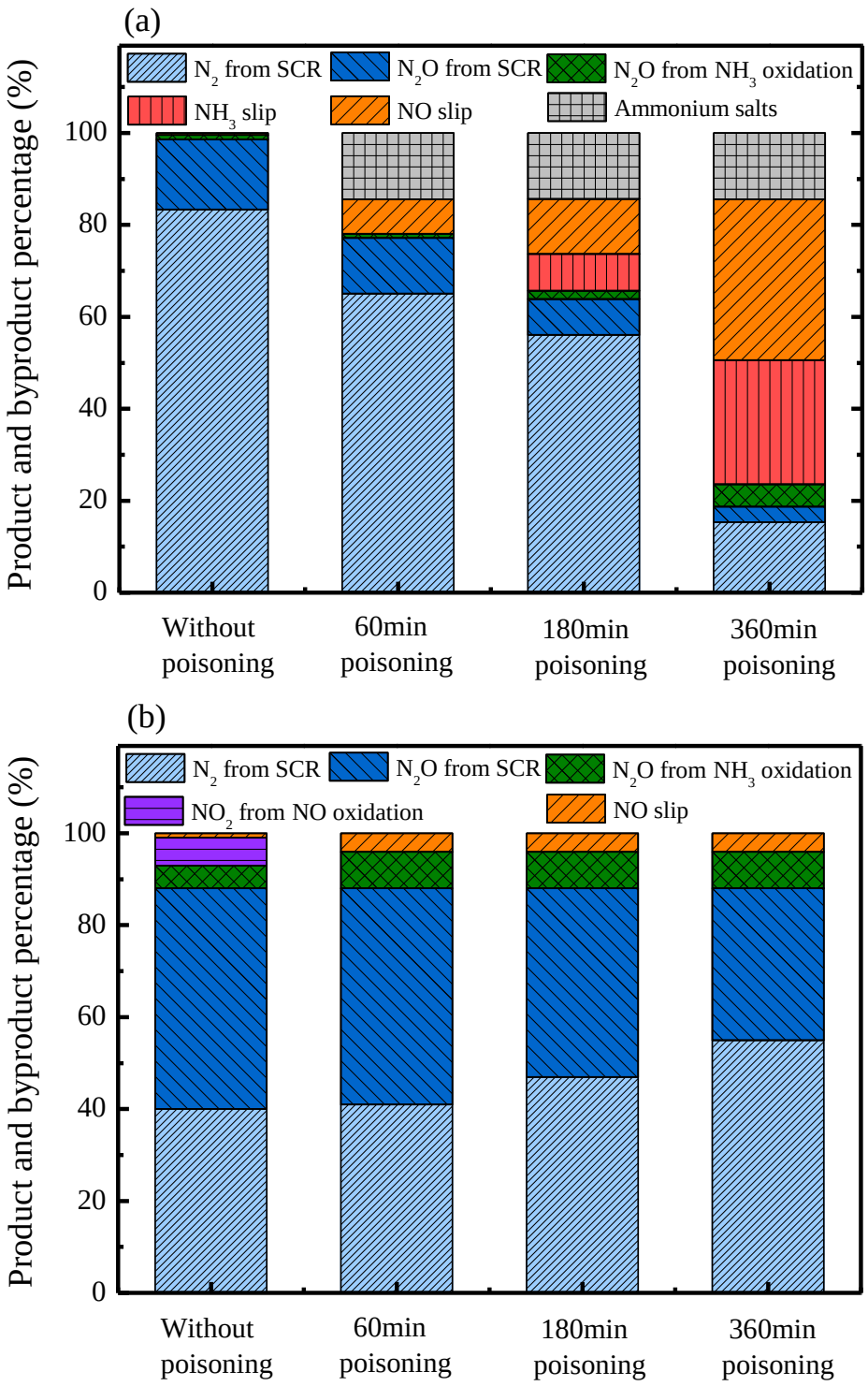

Figure 7. Product and byproduct percentages of N-containing species during the SCR process over $MnFe/TiO_2$ catalyst with SO_2 poisoning at (**a**) 150 °C and (**b**) 300 °C. The inlet NH_3 and NO molar concentration ratio was 1:1; and the percentage calculation formulas were based on those listed in Table 3.

2.5. Reaction Pathways

From the above results, one could surmise the reaction pathway in the NH_3-SCR system with/without SO_2 at 150 °C and 300 °C as shown in Figure 8. When the SCR system was at 150 °C without SO_2, it can be seen from the top left plot that a fraction of NH_3 and NO would be oxidized to

N_2O and NO_2, respectively. In addition, the major reaction product of SCR reaction was N_2 instead of N_2O. On the other hand, when increasing temperature to 300 °C, it can be seen from the bottom left plot that NH_3 would be oxidized to both N_2O and NO. Moreover, the major reaction product of SCR reaction was N_2O instead of N_2, which was revealed by the low N_2-selectivity as seen in Figure 7b.

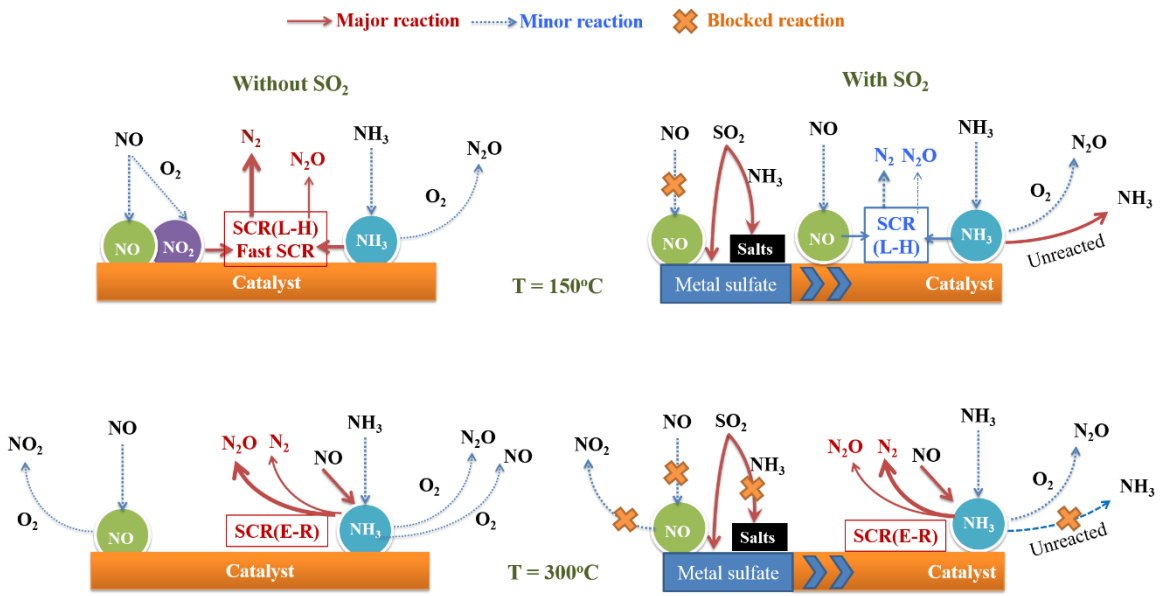

Figure 8. Proposed reaction pathway in the NH_3-SCR system with/without SO_2 at 150 °C and 300 °C. The reaction pathway was based on inlet NH_3 and NO molar concentration ratio of 1:1.

When SO_2 was introduced at 150 °C, it can be seen from the top right plot of Figure 8 that SO_2 would be reacted with both NH_3 and metal catalyst, which resulted in the formation of ammonium salts and metal sulfates, respectively. In addition, because NO could not be adsorbed on metal sulfates, therefore it could not be reacted with NH_3 at low temperature. As a result, unreacted NH_3 (NH_3 slip) turned out to be the major N-containing species in addition to the unreacted NO.

When increasing temperature to 300 °C, it can be seen from the bottom right plot that ammonium salts would not be formed in the presence of SO_2, but SO_2 would react with metal catalyst to form metal sulfates. In addition, gaseous NO could directly react with adsorbed ammonia via Eley−Rideal mechanism [29]. The major reaction product of SCR reaction gradually changed from N_2O to N_2 after increasing poisoning time.

3. Materials and Method

3.1. Reactions in SCR System

In the SCR system, it may contain oxidation reactions, SCR reactions and SO_2 poisoning reactions [46–52].

NH_3 oxidation:

$$2NH_3 + 2O_2 \rightarrow N_2O + 3H_2O \quad (3)$$

$$4NH_3 + 5O_2 \rightarrow 4NO + 6H_2O \quad (4)$$

NO oxidation:

$$2NO + O_2 \rightarrow 2NO_2 \quad (5)$$

SCR reactions:

$$4NO + 4NH_3 + O_2 \rightarrow 4N_2 + 6H_2O \quad (6)$$

$$4NO + 4NH_3 + 3O_2 \rightarrow 4N_2O + 6H_2O \quad (7)$$

$$NO + NO_2 + 2NH_3 \rightarrow 2N_2 + 3H_2O \text{ (fast SCR)} \quad (8)$$

SO_2 oxidation and poisoning:

$$SO_2 + {}^1/_2\, O_2 \rightarrow SO_3 \quad (9)$$

$$SO_3 + 2NH_3 + H_2O \rightarrow (NH_4)_2SO_4 \quad (10)$$

$$SO_3 + NH_3 + H_2O \rightarrow NH_4HSO_4 \quad (11)$$

$$SO_2 + \text{metal} \rightarrow \text{metal sulfates (e.g., } MnSO_4 \text{ and } Ti(SO_4)_2) \quad (12)$$

In this study, experimental tests were designed to clarify the products and byproducts of the above reactions.

3.2. Synthesis of MnFe/TiO$_2$ Catalysts

Mn and Fe metal oxides were supported on TiO_2 (in the form of $TiO(OH)_2$) by the co-precipitation method. In a typical procedure, 8 g of TiO_2 (China Steel Corp., Kaohsiung, Taiwan), 11.57 g of ferric nitrate 9-hydrate (99%,J.T. Baker, Radnor, PA, USA), 7.13 g of manganese (II) acetate tetrahydrate (99%, Merck, Kenilworth, NJ, USA) and D.I. water (76 g) were mixed then adjusted to pH = 10 with 25 wt.% ammonia solution to form a precipitate. It was filtered and washed thoroughly with D.I. water, then dried at 120 °C for 12 h. Finally, the material was calcined at 350 °C for 6 h in air.

3.3. Catalyst Reaction

The NH_3 oxidation, NO oxidation and SCR activity tests were carried out at atmospheric pressure in a fixed-bed reactor loaded with sieved pelletized (16–30 mesh) catalysts. The operation conditions of inlet gas concentrations, reaction temperatures, and gas hourly space velocity for different tests are shown in Table 3. Under typical NH_3 oxidation, NO oxidation, and SCR reaction tests, the concentrations of NH_3 and/or NO were the same at 500 ppmv, and the SO_2 concentration was 150 ppmv if SO_2 poisoning effect was considered. The feed gases were mixed in a gas mixer. Then the catalysts were preheated in the reactor for 30 min to ensure that an isothermal reaction temperature was reached. During the oxidation and SCR test, the NO and SO_2 concentrations at the inlet and outlet of the reactor were monitored by a NO/SO_2 analyzer (Ultramat 23, SIEMENS, Munich, Germany). In addition, the concentrations of NH_3, N_2O, and NO_2 at the inlet and outlet of the reactor were monitored by a FTIR Spectrophotometer (Bomem MB 104,San Jose, CA, USA and ITRI, Hsinchu, Taiwan).

Table 3. Operation conditions of experimental tests in this study.

	NH_3 (ppmv)	NO (ppmv)	SO_2 (ppmv)	O_2 (%)	Temperature (°C)	GHSV (hr^{-1})
NH_3 oxidation test	500	0	0	10%	100–300	50,000
NO oxidation test	0	500	0	10%	100–300	50,000
SCR test without SO_2	500	500	0	10%	100–300	50,000
SCR test with SO_2	500	500	150	10%	150 & 300	50,000
SCR test with SO_2 at different NH_3 amounts	500–600	500	150	10%	150	50,000

The NO consumption due to SCR reactions (Equations (6)–(8)) must be subtracted by the NO oxidation to NO_2 (Equation (5)). Thus, the NO consumption of SCR, $[NO]_{SCR}$ is defined by:

$$[NO]_{SCR} = [NO]_{in} - ([NO]_{out} - [NO_2]_{out}) \quad (13)$$

Since the N-containing product and byproduct of SCR reaction are N_2 and N_2O from Equations (6)–(8), thus the N_2-selectivity of SCR reactions was calculated by

$$N_2 \text{ selectivity of SCR reaction } = \left[1 - \frac{[NO]_{out} + [NH_3]_{out} + [N_2O]_{out} + [NO_2]_{out}}{[NO]_{in} + [NH_3]_{in}}\right] \times 100\% \quad (14)$$

The TGA was conducted to determine the sulfates species forming on the surface of the catalysts with a NETZSCH TG 209 F1 apparatus. The heating program was carried out under airflow of 10 mL/min with a heating rate of 10 °C/min from room temperature to 900 °C.

4. Conclusions

This study employed $MnFe/TiO_2$ catalyst to study the product/byproducts for the oxidation of NH_3, the oxidation of NO and the NH_3-SCR reaction with/without SO_2 to understand the reaction pathway of medium to low-temperature SCR process. For SCR operation temperature of 150 °C without the presence of SO_2, the major product of SCR process appeared to be N_2. The minor presence of N_2O byproduct was majorly from the SCR reaction instead of from the NH_3 oxidation reaction. Moreover, the result indicated that products of the SCR reaction gradually changed from N_2 to N_2O when raising the temperature from 100 to 300 °C. Therefore, the N_2-selectivity of SCR reaction was gradually decreased. One the other hand when SO_2 was introduced at 150 °C, the percentages of N_2 and N_2O decreased after increased poisoning time. However, when increasing temperature to 300 °C, the percentages of N_2 increased while that of N_2O decreased after increasing the poisoning time. This indicated the existence of SO_2 promotion effect on the NH_3-SCR at 300 °C.

Author Contributions: Conceptualization, T.L. and H.B.; methodology, T.L. and H.B.; validation, H.B.; formal analysis, T.L.; investigation, T.L.; resources, H.B.; data curation, T.L. and H.B.; writing—original draft preparation, T.L.; writing—review and editing, H.B.; visualization, T.L. and H.B.; supervision, H.B.; project administration, H.B.; funding acquisition, H.B.

Funding: This research received no external funding.

Acknowledgments: The authors gratefully acknowledge the financial support from the Ministry of Science and Technology, Taiwan through grant No: MOST 105-3113-E-009-003.

Conflicts of Interest: The authors declare no conflict of interest.

References

1. Busca, G.; Lietti, L.; Ramis, G.; Berti, F. Chemical and mechanistic aspects of the selective catalytic reduction of NO_x by ammonia over oxide catalysts: A review. *Appl. Catal. B Environ.* **1998**, *18*, 1–36. [CrossRef]
2. Chang, Y.Y.; Yan, Y.L.; Tseng, C.H.; Syu, J.Y.; Lin, W.Y.; Yuan, Y.C. Development of an Innovative Circulating Fluidized-Bed with Microwave System for Controlling NO_x. *Aerosol Air Qual. Res.* **2012**, *12*, 379–386. [CrossRef]
3. Garcia-Bordeje, E.; Pinilla, J.L.; Lazaro, M.J.; Moliner, R.; Fierro, J.L.G. Role of sulphates on the mechanism of NH_3-SCR of NO at low temperatures over presulphated vanadium supported on carbon-coated monoliths. *J. Catal.* **2005**, *233*, 166–175. [CrossRef]
4. Gan, L.N.; Guo, F.; Yu, J.; Xu, G.W. Improved Low-Temperature Activity of V_2O_5-WO_3/TiO_2 for Denitration Using Different Vanadium Precursors. *Catalysts* **2016**, *6*, 25. [CrossRef]
5. Kompio, P.G.W.A.; Bruckner, A.; Hipler, F.; Auer, G.; Loffler, E.; Grunert, W. A new view on the relations between tungsten and vanadium in V_2O_5-WO_3/TiO_2 catalysts for the selective reduction of NO with NH_3. *J. Catal.* **2012**, *286*, 237–247. [CrossRef]
6. Krocher, O. Selective Catalytic Reduction of NO_x. *Catalysts* **2018**, *8*, 459. [CrossRef]
7. Balle, P.; Geiger, B.; Kureti, S. Selective catalytic reduction of NO_x by NH_3 on Fe/HBEA zeolite catalysts in oxygen-rich exhaust. *Appl. Catal. B Environ.* **2009**, *85*, 109–119. [CrossRef]
8. Kim, M.H.; Yang, K.H. The Role of Fe_2O_3 Species in Depressing the Formation of N_2O in the Selective Reduction of NO by NH_3 over V_2O_5/TiO_2-Based Catalysts. *Catalysts* **2018**, *8*, 134.

9. Lee, S.M.; Kim, S.S.; Hong, S.C. Systematic mechanism study of the high temperature SCR of NO_x by NH_3 over a W/TiO_2 catalyst. *Chem. Eng. Sci.* **2012**, *79*, 177–185.
10. Ning, R.; Chen, L.; Li, E.; Liu, X.; Zhu, T. Applicability of V_2O_5-WO_3/TiO_2 Catalysts for the SCR Denitrification of Alumina Calcining Flue Gas. *Catalysts* **2019**, *9*, 220. [CrossRef]
11. Gao, R.H.; Zhang, D.S.; Liu, X.G.; Shi, L.Y.; Maitarad, P.; Li, H.R.; Zhang, J.P.; Cao, W.G. Enhanced catalytic performance of V_2O_5-$WO_3/Fe_2O_3/TiO_2$ microspheres for selective catalytic reduction of NO by NH_3. *Catal. Sci. Technol.* **2013**, *3*, 191–199. [CrossRef]
12. Xu, W.Q.; He, H.; Yu, Y.B. Deactivation of a Ce/TiO_2 Catalyst by SO_2 in the Selective Catalytic Reduction of NO by NH_3. *J. Phys. Chem. C* **2009**, *113*, 4426–4432. [CrossRef]
13. Yang, R.; Huang, H.F.; Chen, Y.J.; Zhang, X.X.; Lu, H.F. Performance of Cr-doped vanadia/titania catalysts for low-temperature selective catalytic reduction of NO_x with NH_3. *Chin. J. Catal.* **2015**, *36*, 1256–1262. [CrossRef]
14. Kong, Z.J.; Wang, C.; Ding, Z.N.; Chen, Y.F.; Zhang, Z.K. Enhanced activity of $Mn_xW_{0.05}Ti_{0.95-x}O_{2-\delta}$ for selective catalytic reduction of NO_x with ammonia by self-propagating high-temperature synthesis. *Catal. Commun.* **2015**, *64*, 27–31. [CrossRef]
15. Lian, Z.H.; Liu, F.D.; He, H.; Shi, X.Y.; Mo, J.S.; Wu, Z.B. Manganese-niobium mixed oxide catalyst for the selective catalytic reduction of NO_x with NH_3 at low temperatures. *Chem. Eng. J.* **2014**, *250*, 390–398. [CrossRef]
16. Gao, C.; Shi, J.W.; Fan, Z.Y.; Gao, G.; Niu, C.M. Sulfur and Water Resistance of Mn-Based Catalysts for Low-Temperature Selective Catalytic Reduction of NO_x: A Review. *Catalysts* **2018**, *8*, 11. [CrossRef]
17. Putluru, S.S.R.; Schill, L.; Godiksen, A.; Poreddy, R.; Mossin, S.; Jensen, A.D.; Fehrmann, R. Promoted V_2O_5/TiO_2 catalysts for selective catalytic reduction of NO with NH_3 at low temperatures. *Appl. Catal. B Environ.* **2016**, *183*, 282–290. [CrossRef]
18. Gil, S.; Garcia-Vargas, J.M.; Liotta, L.F.; Pantaleo, G.; Ousmane, M.; Retailleau, L.; Giroir-Fendler, A. Catalytic Oxidation of Propene over Pd Catalysts Supported on CeO_2, TiO_2, Al_2O_3 and M/Al_2O_3 Oxides (M = Ce, Ti, Fe, Mn). *Catalysts* **2015**, *5*, 671–689. [CrossRef]
19. Liu, L.; Gao, X.; Song, H.; Zheng, C.H.; Zhu, X.B.; Luo, Z.Y.; Ni, M.J.; Cen, K.F. Study of the Promotion Effect of Iron on Supported Manganese Catalysts for No Oxidation. *Aerosol Air Qual. Res.* **2014**, *14*, 1038–1046. [CrossRef]
20. Shi, J.; Zhang, Z.H.; Chen, M.X.; Zhang, Z.X.; Shangguan, W.F. Promotion effect of tungsten and iron co-addition on the catalytic performance of MnO_x/TiO_2 for NH_3-SCR of NOx. *Fuel* **2017**, *210*, 783–789. [CrossRef]
21. Zhu, L.; Zhong, Z.P.; Yang, H.; Wang, C.H. NH_3-SCR Performance of Mn-Fe/TiO_2 Catalysts at Low Temperature in the Absence and Presence of Water Vapor. *Water Air Soil Poll.* **2016**, *227*, 476. [CrossRef]
22. Deng, S.C.; Zhuang, K.; Xu, B.L.; Ding, Y.H.; Yu, L.; Fan, Y.N. Promotional effect of iron oxide on the catalytic properties of Fe-MnO_x/TiO_2 (anatase) catalysts for the SCR reaction at low temperatures. *Catal. Sci. Technol.* **2016**, *6*, 1772–1778. [CrossRef]
23. Dong, L.F.; Fan, Y.M.; Ling, W.; Yang, C.; Huang, B.C. Effect of Ce/Y Addition on Low-Temperature SCR Activity and SO_2 and H_2O Resistance of MnO_x/ZrO_2/MWCNTs Catalysts. *Catalysts* **2017**, *7*, 181. [CrossRef]
24. Mu, W.T.; Zhu, J.; Zhang, S.; Guo, Y.Y.; Su, L.Q.; Li, X.Y.; Li, Z. Novel proposition on mechanism aspects over Fe-Mn/ZSM-5 catalyst for NH_3-SCR of NO_x at low temperature: Rate and direction of multifunctional electron-transfer-bridge and in situ DRIFTs analysis. *Catal. Sci. Technol.* **2016**, *6*, 7532–7548. [CrossRef]
25. Chen, T.; Guan, B.; Lin, H.; Zhu, L. In situ DRIFTS study of the mechanism of low temperature selective catalytic reduction over manganese-iron oxides. *Chin. J. Catal.* **2014**, *35*, 294–301. [CrossRef]
26. Zhou, G.Y.; Zhong, B.C.; Wang, W.H.; Guan, X.J.; Huang, B.C.; Ye, D.Q.; Wu, H.J. In situ DRIFTS study of NO reduction by NH_3 over Fe-Ce-Mn/ZSM-5 catalysts. *Catal. Today* **2011**, *175*, 157–163. [CrossRef]
27. Lin, Q.C.; Li, J.H.; Ma, L.; Hao, J.M. Selective catalytic reduction of NO with NH_3 over Mn-Fe/USY under lean burn conditions. *Catal. Today* **2010**, *151*, 251–256. [CrossRef]
28. Zhang, K.; Yu, F.; Zhu, M.Y.; Dan, J.M.; Wang, X.G.; Zhang, J.L.; Dai, B. Enhanced Low Temperature NO Reduction Performance via MnO_x-Fe_2O_3/Vermiculite Monolithic Honeycomb Catalysts. *Catalysts* **2018**, *8*, 100. [CrossRef]

29. Liu, F.D.; He, H.; Ding, Y.; Zhang, C.B. Effect of manganese substitution on the structure and activity of iron titanate catalyst for the selective catalytic reduction of NO with NH_3. *Appl. Catal. B Environ.* **2009**, *93*, 194–204. [CrossRef]
30. Shu, Y.; Sun, H.; Quan, X.; Chen, S.O. Enhancement of Catalytic Activity Over the Iron-Modified Ce/TiO_2 Catalyst for Selective Catalytic Reduction of NO_x with Ammonia. *J. Phys. Chem. C* **2012**, *116*, 25319–25327. [CrossRef]
31. Yang, S.J.; Xiong, S.C.; Liao, Y.; Xiao, X.; Qi, F.H.; Peng, Y.; Fu, Y.W.; Shan, W.P.; Li, J.H. Mechanism of N_2O Formation during the Low-Temperature Selective Catalytic Reduction of NO with NH_3 over Mn-Fe Spinel. *Environ. Sci. Technol.* **2014**, *48*, 10354–10362. [CrossRef] [PubMed]
32. Lee, T.Y.; Liou, S.Y.; Bai, H.L. Comparison of titania nanotubes and titanium dioxide as supports of low-temperature selective catalytic reduction catalysts under sulfur dioxide poisoning. *J. Air Waste Manag.* **2017**, *67*, 292–305. [CrossRef] [PubMed]
33. Tuenter, G.; Vanleeuwen, W.F.; Snepvangers, L.J.M. Kinetics and Mechanism of the NO_x Reduction with NH_3 on V_2O_5-WO_3-TiO_2 Catalyst. *Ind. Eng. Chem. Prod. Res. Dev.* **1986**, *25*, 633–636. [CrossRef]
34. Kang, M.; Park, E.D.; Kim, J.M.; Yie, J.E. Manganese oxide catalysts for NO_x reduction with NH_3 at low temperatures. *Appl. Catal. A Gen.* **2007**, *327*, 261–269. [CrossRef]
35. Ruggeri, M.P.; Grossale, A.; Nova, I.; Tronconi, E.; Jirglova, H.; Sobalik, Z. FTIR in situ mechanistic study of the NH_3-NO/NO_2 "Fast SCR" reaction over a commercial Fe-ZSM-5 catalyst. *Catal. Today* **2012**, *184*, 107–114. [CrossRef]
36. Park, K.H.; Lee, S.M.; Kim, S.S.; Kwon, D.W.; Hong, S.C. Reversibility of Mn Valence State in MnO_x/TiO_2 Catalysts for Low-temperature Selective Catalytic Reduction for NO with NH_3. *Catal. Lett.* **2013**, *143*, 246–253. [CrossRef]
37. Cao, F.; Xiang, J.; Su, S.; Wang, P.Y.; Hu, S.; Sun, L.S. Ag modified Mn-Ce/gamma-Al_2O_3 catalyst for selective catalytic reduction of NO with NH_3 at low-temperature. *Fuel Process. Technol.* **2015**, *135*, 66–72. [CrossRef]
38. Xu, H.D.; Fang, Z.T.; Cao, Y.; Kong, S.; Lin, T.; Gong, M.C.; Chen, Y.Q. Influence of Mn/(Mn plus Ce) Ratio of MnO_x-CeO_2/WO_3-ZrO_2 Monolith Catalyst on Selective Catalytic Reduction of NO_x with Ammonia. *Chin. J. Catal.* **2012**, *33*, 1927–1937. [CrossRef]
39. Liu, F.D.; Asakura, K.; He, H.; Shan, W.P.; Shi, X.Y.; Zhang, C.B. Influence of sulfation on iron titanate catalyst for the selective catalytic reduction of NO_x with NH_3. *Appl. Catal. B Environ.* **2011**, *103*, 369–377. [CrossRef]
40. Shu, Y.; Aikebaier, T.; Quan, X.; Chen, S.; Yu, H.T. Selective catalytic reaction of NO_x with NH_3 over Ce-Fe/TiO_2-loaded wire-mesh honeycomb: Resistance to SO_2 poisoning. *Appl. Catal. B Environ.* **2014**, *150*, 630–635. [CrossRef]
41. Zhang, L.F.; Zhang, X.L.; Lv, S.S.; Wu, X.P.; Wang, P.M. Promoted performance of a MnO_x/PG catalyst for low-temperature SCR against SO_2 poisoning by addition of cerium oxide. *RSC Adv.* **2015**, *5*, 82952–82959. [CrossRef]
42. Pourkhalil, M.; Moghaddam, A.Z.; Rashidi, A.; Towfighi, J.; Mortazavi, Y. Preparation of highly active manganese oxides supported on functionalized MWNTs for low temperature NO_x reduction with NH_3. *Appl. Surf. Sci.* **2013**, *279*, 250–259. [CrossRef]
43. Wang, X.B.; Gui, K.T. Fe_2O_3 particles as superior catalysts for low temperature selective catalytic reduction of NO with NH_3. *J. Environ. Sci.* **2013**, *25*, 2469–2475. [CrossRef]
44. Jin, R.B.; Liu, Y.; Wang, Y.; Cen, W.L.; Wu, Z.B.; Wang, H.Q.; Weng, X.L. The role of cerium in the improved SO_2 tolerance for NO reduction with NH_3 over Mn-Ce/TiO_2 catalyst at low temperature. *Appl. Catal. B Environ.* **2014**, *148*, 582–588. [CrossRef]
45. Shen, B.X.; Zhang, X.P.; Ma, H.Q.; Yao, Y.; Liu, T. A comparative study of Mn/CeO_2, Mn/ZrO_2 and Mn/Ce-ZrO_2 for low temperature selective catalytic reduction of NO with NH_3 in the presence of SO_2 and H_2O. *J. Environ. Sci. China* **2013**, *25*, 791–800. [CrossRef]
46. Lee, T.; Bai, H. Metal Sulfate Poisoning Effects over MnFe/TiO_2 for Selective Catalytic Reduction of NO by NH_3 at Low Temperature. *Ind. Eng. Chem. Res.* **2018**, *57*, 4848–4858. [CrossRef]
47. Busca, G.; Larrubia, M.A.; Arrighi, L.; Ramis, G. Catalytic abatement of NO_x: Chemical and mechanistic aspects. *Catal. Today* **2005**, *107–108*, 139–148. [CrossRef]
48. Kapteijn, F.; Singoredjo, L.; Andreini, A.; Moulijn, J.A. Activity and Selectivity of Pure Manganese Oxides in the Selective Catalytic Reduction of Nitric-Oxide with Ammonia. *Appl. Catal. B Environ.* **1994**, *3*, 173–189. [CrossRef]

49. Wang, Y.L.; Li, X.X.; Zhan, L.; Li, C.; Qiao, W.M.; Ling, L.C. Effect of SO_2 on Activated Carbon Honeycomb Supported CeO_2-MnO_x Catalyst for NO Removal at Low Temperature. *Ind. Eng. Chem. Res.* **2015**, *54*, 2274–2278. [CrossRef]
50. Yang, W.W.; Liu, F.D.; Xie, L.J.; Lan, Z.H.; He, H. Effect of V_2O_5 Additive on the SO_2 Resistance of a Fe_2O_3/AC Catalyst for NH_3-SCR of NO_x at Low Temperatures. *Ind. Eng. Chem. Res.* **2016**, *55*, 2677–2685. [CrossRef]
51. Qiu, L.; Wang, Y.; Pang, D.D.; Ouyang, F.; Zhang, C.L.; Cao, G. Characterization and Catalytic Activity of Mn-Co/TiO_2 Catalysts for NO Oxidation to NO_2 at Low Temperature. *Catalysts* **2016**, *6*, 9. [CrossRef]
52. Lippits, M.J.; Gluhoi, A.C.; Nieuwenhuys, B.E. A comparative study of the selective oxidation of NH_3 to N_2 over gold, silver and copper catalysts and the effect of addition of Li_2O and CeO_x. *Catal. Today* **2008**, *137*, 446–452. [CrossRef]